

# A study of the phase transition in the transverse Ising model using the extended coupled-cluster method

J. Rosenfeld

*IRST-SSI, Loc. Pante' di Povo, I-38100 Povo (Trento), Italy*

N.E. Ligterink \*

*ECT\*, Villa Tambosi, Strada delle Tabarelle 286, I-38050 Villazzano (Trento), Italy*

(October 7, 2018)

The phase transition present in the linear-chain and square-lattice cases of the transverse Ising model is examined. The extended coupled cluster method (ECCM) can describe both sides of the phase transition with a unified approach. The correlation length and the excitation energy are determined. We demonstrate the ability of the ECCM to use both the weak- and the strong-coupling starting state in a unified approach for the study of critical behavior.

## I. INTRODUCTION

The study of the magnetic properties of materials from microscopic theory has always proved difficult. Even at the level of such simplified magnetic models as the Heisenberg model, the Ising model, and the Hubbard model, intensive theoretical and numerical work is required to model the interesting counter-intuitive behavior they exhibit.

An obstacle to studying quantum magnets, encountered by various theoretical approaches, is due to the uniqueness of the state at the phase transition point. Most techniques can describe a particular phase of a quantum magnet but may be unable to describe the other phase, or phases, of the system and, hence, the phase transition itself. Clearly, a consequence for such techniques is that conclusive evidence of symmetry breaking cannot be found.

All techniques dealing with many-body systems experience the difficulty of being able to include sufficient correlations, without making prior assumptions about the leading correlations, in order to provide a good description of the important behavior of the system. Unsurprisingly, the subtleties of a quantum magnet at the phase transition, which require the inclusion of a great many correlations to model adequately, are notoriously difficult to obtain. Many theoretical approaches [1] yield a mean-field like description of the system, which does not reveal the distinctly different behavior present in differing dimensions, contrary to the true physical behavior. [2]

In this paper, we present a study of the transverse Ising model via an improved approach [3,4] recently developed for spin systems. This approach involves the application of the quantum many-body technique known as the extended coupled-cluster method (ECCM). *A priori*, we know that the ECCM is potentially a good technique for studying the phase transition as it possesses certain features that allow it to study spontaneous symmetry breaking. In particular, the ECCM can yield a single solution that correctly describes the physical behavior on either side of the phase transition. The more widely applied normal coupled-cluster method (NCCM), which is a restricted version of the ECCM, at a given level of approximation, does not possess this feature of the ECCM. A comparison of the results from these techniques will demonstrate the superiority of the ECCM with regard to the study of the phase transition. Most importantly, we aim to show that the improved approach outlined in [4] yields trustworthy and accurate numerical data that can provide real insight into the physical behavior of the system.

The transverse Ising model has two distinct phases; the ferromagnetic phase, and the paramagnetic phase, which are tuned by a single coupling constant. On the linear chain, this model has some interesting properties, such as the duality, which allows one to relate the ground-state energy at a particular value of the coupling constant to the ground-state energy at the reciprocal value of the coupling constant. This property and the fact the model is exactly solvable on the linear chain makes it a good test-ground for the ECCM. With the confidence gained from the linear-chain model, we will then study the square-lattice case.

---

\*e-mail: ligterin@ect.it

## II. THE TRANSVERSE ISING MODEL

The transverse Ising Hamiltonian has two competing terms on a lattice composed of spin-half spins; the ferromagnetic term, which forces the system to align in the  $z$ -direction, and the paramagnetic term, which forces the system to align along the positive  $x$ -axis:

$$H = - \sum_{\langle \mathbf{i}, \mathbf{j} \rangle} \sigma_{\mathbf{i}}^z \sigma_{\mathbf{j}}^z - \lambda \sum_{\mathbf{i}} \sigma_{\mathbf{i}}^x \quad , \quad (2.1)$$

where  $\sigma^i$  are the Pauli matrices,  $\lambda$  is the external magnetic field,  $N$  is the number of lattice sites,  $d$  the dimensionality of the lattice, and the sum over  $\langle \mathbf{i}, \mathbf{j} \rangle$  runs over all nearest-neighbor pairs of lattice sites  $\mathbf{i}$  and  $\mathbf{j}$ . In the weak-coupling limit,  $\lambda = 0$ , the spins will align themselves along the  $z$ -axis, in either the positive or the negative direction. In the strong-coupling limit,  $\lambda \rightarrow \infty$ , the magnetic field forces the spins to align along the positive  $x$ -axis. Between these two phases a phase transition occurs for some critical coupling  $\lambda_c$ .

Starting from the strong-coupling limit, the  $Z(2)$  symmetry is preserved, which results in the  $\langle \sigma^z \rangle = M^z$  being zero. Beyond the critical point this symmetry is broken, and two degenerate ground states exist, with  $\pm M^z$ . Any *ab-initio* method would have difficulties in breaking such a symmetry. We will show that within a specific approximation, we can start with an uncorrelated model state in both limits, which can either incorporate the  $Z(2)$  symmetry or break it, in the latter case two exactly degenerate states exist.

### A. Exact results on the linear chain

On the linear chain the model is exactly solvable. [5,6] After a Jordan-Wigner transformation the Hamiltonian can be diagonalized using a Bogoliubov transformation. The ground-state energy is given by:

$$\begin{aligned} \frac{E_g(\lambda)}{N} &= -\frac{1}{\pi} \int_0^\pi dq \sqrt{1 + 2\lambda \cos q + \lambda^2} \\ &= -\frac{2}{\pi} (1 + \lambda) \mathcal{E} \left( \frac{4\lambda}{(1 + \lambda)^2} \right) \quad , \end{aligned} \quad (2.2)$$

where  $\mathcal{E}$  is a complete elliptic integral of the second kind. This energy satisfies the interesting duality, as could be concluded from the duality of the original Hamiltonian:

$$E_g(\lambda) = \lambda E_g(\lambda^{-1}) \quad . \quad (2.3)$$

The magnetization  $M^\alpha = \langle \sigma^\alpha \rangle$  is given by:

$$M^x = \frac{1}{\pi} \int_0^\pi \frac{(\lambda + \cos q) dq}{\sqrt{1 + 2\lambda \cos q + \lambda^2}} \quad , \quad (2.4)$$

$$M^z = \theta(1 - \lambda) (1 - \lambda^2)^{\frac{1}{8}} \quad , \quad (2.5)$$

where  $\theta(x)$  is the step function;  $\theta(x < 0) = 0$  and  $\theta(x > 0) = 1$ . The transverse magnetization  $M^x$  can be related to the derivative of the ground-state energy, however, the longitudinal magnetization  $M^z$  is derived from the limit of the spin-spin correlation function with a lattice size taken to infinity, therefore the vanishing long-range order for  $\lambda > 1$  is a subtle result. [5]

### B. The mean field

A parameterization of the wave function is given by:

$$|\Psi\rangle = \left| \left( \begin{array}{c} -\sin \theta/2 \\ \cos \theta/2 \end{array} \right), \left( \begin{array}{c} -\sin \theta/2 \\ \cos \theta/2 \end{array} \right), \left( \begin{array}{c} -\sin \theta/2 \\ \cos \theta/2 \end{array} \right), \left( \begin{array}{c} -\sin \theta/2 \\ \cos \theta/2 \end{array} \right), \dots \right\rangle \quad . \quad (2.6)$$

From the variational principle the mean-field solution yields:

$$\theta = -\arcsin \bar{\lambda} \ ; \ \bar{\lambda} \leq 1 \ , \quad (2.7)$$

$$= -\frac{\pi}{2} \ ; \ \bar{\lambda} \geq 1 \ , \quad (2.8)$$

$$\frac{E_g}{N} = -d(1 + \bar{\lambda}^2) \ ; \ \bar{\lambda} \leq 1 \ , \quad (2.9)$$

$$= -2d\bar{\lambda} \ ; \ \bar{\lambda} \geq 1 \ , \quad (2.10)$$

$$M^z = \theta(1 - \bar{\lambda})\sqrt{1 - \bar{\lambda}^2} \ , \quad (2.11)$$

where  $\lambda = 2d\bar{\lambda}$ . Note that  $\theta \rightarrow -\pi - \theta$  is also a solution with the same energy but opposite magnetization. This is the  $Z(2)$  symmetry partner of the ferromagnetic ground state.

### III. THE EXTENDED-COUPLED CLUSTER METHOD

The Coupled-Cluster Method (CCM) which exists in two distinct versions, the NCCM and the ECCM, is a powerful technique for quantum many-body calculations. Only the essential features of the CCM will be reviewed here, further details can be found in the literature. [7,8,4] There are four key features of the CCM. Firstly, the model state  $|\Phi\rangle$ , an uncorrelated state, which is usually the true ground state in a certain limit, serves as the starting state. Secondly, the correlations are incorporated in the ket state in the exponentiated form:

$$|\Psi\rangle = e^S|\Phi\rangle \ , \quad (3.1)$$

where the correlation operator  $S$  is composed solely of a complete set of mutually commuting multiconfigurational creation operators that annihilate the bra model state  $\langle\Phi|$ . The exponential form ensures the correct summation of the independent correlations in the calculation, and spreads correlations over the whole system although the correlations in  $S$  might be only local.

The third key feature of the CCM appears in the parameterization of the bra state  $\langle\tilde{\Psi}|$ ,

$$\langle\tilde{\Psi}| = \langle\Phi|(1 + \tilde{S})e^{-S} = \langle\Phi|e^{S''}e^{-S} \ , \quad (3.2)$$

where the first parameterization gives rise to the NCCM, and the second parameterization gives rise to the ECCM. [7] The importance of both of the above bra-state parameterizations are that they allow the similarity transform to be incorporated into the CCM calculation of any observable. Primarily, the similarity transform only yields terms for which the correlations present in  $S$  are linked to the observable, and, hence, subsequent expectation values are size-extensive quantities. Importantly, the presence of the similarity transform means that no further truncations are necessary than the truncations of the number of configuration of creation operators in  $S$ . In this way the similarity transform can be seen as the defining feature of the CCM, since its absence would render an approximate calculation impractical. For example, if one would attempt a variational calculation with the ket state of Eq. (3.1) and its Hermitian conjugate, several further approximations are required to calculate the functional. Therefore, the actual ket state obtained from the same parameterized variational wave functional depends on the associated bra state and the corresponding variational principle.

This brings us to the fourth key feature of the CCM, which is related to the parameterization of the bra state in Eq. (3.2) and concerns the terms arising from  $e^{S''}$  and  $\tilde{S}$ . These terms are present in the ECCM and NCCM respectively and are solely composed of destruction operators; the Hermitian conjugates of the creation operators in  $S$ . Therefore, the functional  $\langle\tilde{\Psi}|H|\Psi\rangle$  is a polynomial in the bra and ket coefficients, associated with the strength of the different creation and annihilation operators in  $S$  and  $S''$  respectively. [7]

Both of the NCCM and ECCM parameterizations result in the maintenance of some useful formal properties, which remain valid in any approximation scheme, e.g., Feynman-Hellman theorem and the linked-cluster theorem for the ket state coefficients. [8] However, the ECCM, unlike the NCCM, parameterization retains, in any approximation scheme, the full cluster separability:

$$\lim_{|\mathbf{r}-\mathbf{r}'|\rightarrow\infty} \langle A_{\mathbf{r}}B_{\mathbf{r}'} \rangle = \langle A_{\mathbf{r}} \rangle \langle B_{\mathbf{r}'} \rangle \ , \quad (3.3)$$

where  $A_{\mathbf{r}}$  and  $B_{\mathbf{r}'}$  are localized operators acting at positions  $\mathbf{r}$  and  $\mathbf{r}'$ , respectively. Therefore, it allows us to separate the correlation spin-spin function  $\langle\sigma_{\mathbf{r}}^x\sigma_{\mathbf{r}'}^x\rangle$  into a size-extensive part, the long-range order;  $\langle\sigma^x\rangle^2 = (M^x)^2$ , and the true correlation function that vanishes at infinite distance.

### A. Transformation of the Hamiltonian in terms of a canted model state

For a unified description of the different model states  $|\Phi\rangle$ , we perform a unitary transformation such that the model state, which is a mean field state where the spins point in a particular direction, is a state composed of down-pointing spins. The details of this transformation have been given elsewhere. [3,4] Hence, the creation operators in  $S$  will be products of  $\sigma^+$ 's at different sites. Using the rotation matrix  $U$ , for this purpose, defined by,

$$U \equiv \exp\left(i\theta\frac{\sigma^y}{2}\right) = \cos\left(\frac{\theta}{2}\right)\mathbb{1} + i\sin\left(\frac{\theta}{2}\right)\sigma^y \quad , \quad (3.4)$$

one can obtain the transverse Ising Hamiltonian defined with respect to an arbitrary canted model state, in terms of rotated operators corresponding to the down-spin model state. An illustration of the particular canted states of the ferromagnetic and paramagnetic states, described by the angle  $\theta$ , are respectively given by:

$$\theta = 0 \quad ; \quad |\downarrow\downarrow\downarrow\downarrow\cdots\rangle_{\lambda=0} \quad , \quad \theta = -\pi/2 \quad ; \quad |\rightarrow\rightarrow\rightarrow\rightarrow\cdots\rangle_{\lambda\rightarrow\infty} \quad . \quad (3.5)$$

The rotated transverse Ising Hamiltonian is of the form:

$$\begin{aligned} UHU^\dagger = & - \sum_{\langle i,j \rangle}^{dN} [\sin^2\theta\sigma_i^x\sigma_j^x + \cos^2\theta\sigma_i^z\sigma_j^z + \sin 2\theta\sigma_i^x\sigma_j^z] \\ & - \lambda \sum_i^N [-\sin\theta\sigma_i^z + \cos\theta\sigma_i^x] \quad . \end{aligned} \quad (3.6)$$

In most cases we use only two rotations: the ferromagnetic Hamiltonian, with  $\theta = 0$ , and the paramagnetic Hamiltonian, with  $\theta = -\frac{\pi}{2}$ .

### B. The SUB1 scheme and symmetry breaking

The ECCM SUB1 approximation scheme only retains the one-body correlations present in  $S$  and  $S''$  in Eqs. (3.1) and (3.2) defined with respect to the rotated model state, given by:

$$S = k \sum_i \sigma_i^+ \quad ; \quad S'' = k'' \sum_i \sigma_i^- \quad . \quad (3.7)$$

Performing the CCM SUB1 scheme is equivalent to a mean-field calculation with an important proviso. Crucially, the ECCM SUB1 scheme can yield the full mean-field ground-state solution, however, the NCCM SUB1 scheme can not yield the ground-state solution for the region beyond the phase transition. This feature of the NCCM has dire implications for the study of symmetry breaking. It is a little known fact that, in practice, the CCM yields a solution that preserves the shared symmetry of the model state and the Hamiltonian [9]. Fortunately, via the use of the ECCM SUB1 scheme, it is possible to obtain a symmetry-broken solution in a correlated ECCM calculation.

The relationship between the mean-field ground state and the ECCM one-body coefficients defined with respect to the canted model state, where the spin are rotated downwards, is given by: [3]

$$k = -\tan\left(\frac{\theta}{2}\right) \quad ; \quad k'' = -\frac{1}{2}\sin\theta \quad . \quad (3.8)$$

In a correlated ECCM calculation, these relations are only valid in the classical regimes,  $\lambda = 0$  and  $\lambda = \infty$ , of the system. By using the values of  $k$  and  $k''$ , from Eq. (3.8), starting from an initial point in the classical region of the phase where the chosen model state is not the classical wave function, one can determine the symmetry-broken solution.

The above ansatz is put into practice to study the possibility of broken  $Z(2)$  symmetry in the transverse Ising model. Employing the paramagnetic model state, with the values  $k = 1$  and  $k'' = 1/2$ , which has the advantage of not artificially breaking the  $Z(2)$  symmetry, corresponds to the ferromagnetic state. At the ferromagnetic point  $\lambda = 0$  it yields the symmetry-broken solution. For  $k = 0$  and  $k'' = 0$  the symmetry preserved solution can be determined, for which  $M^z = 0$ , from the limit  $\lambda \rightarrow \infty$ .

### C. The diagrammatic representation of the SUB2- $n$ scheme functional

In order to perform the numerical ECCM calculation efficiently, a diagrammatic [1,4] representation is implemented. The ECCM SUB2- $n$  approximation scheme is implemented here and is described in greater depth in References [7,4]. Essentially, the SUB2- $n$  scheme retains only one and two-body correlations, where the truncated correlation operators are of the form:

$$S = k \sum_{\mathbf{i}} \sigma_{\mathbf{i}}^+ + \sum_{\mathbf{i}, \mathbf{r}}^{\chi \leq n} b_{\chi(\mathbf{r})} \sigma_{\mathbf{i}}^+ \sigma_{\mathbf{i}+\mathbf{r}}^+ , \quad S'' = k'' \sum_{\mathbf{i}} \sigma_{\mathbf{i}}^- + \sum_{\mathbf{i}, \mathbf{r}}^{\chi \leq n} b''_{\chi(\mathbf{r})} \sigma_{\mathbf{i}}^- \sigma_{\mathbf{i}+\mathbf{r}}^- , \quad (3.9)$$

where  $\chi(\mathbf{r})$  yields a label for each vector distinct under lattice symmetries.

The representation of the combinations of operators which give rise to various physical quantities is outlined in Reference [4]. The transverse Ising functional, defined with respect to the ferromagnetic model state arising from the ECCM SUB2- $n$  scheme is diagrammatically expressed in Fig. 1.

### D. The correlation length and the excitation energies

Although the order of the approximation schemes is not sufficient to study the long-distance behavior of the correlation function, we can examine the correlation length:

$$\xi = \frac{1}{N} \langle \sum_{\mathbf{i}, \mathbf{j}} \sigma_{\mathbf{i}}^x \sigma_{\mathbf{j}}^x \rangle - \frac{1}{N^2} \langle \sum_{\mathbf{i}} \sigma_{\mathbf{i}}^x \rangle^2 . \quad (3.10)$$

A similar correlation length for the  $z$ -components of the spins is computationally too involved to be of any practical use. This expression for the  $\xi$  is easily motivated in the linear-chain case, where

$$\langle \sigma_{\mathbf{i}}^x \sigma_{\mathbf{j}}^x \rangle \propto \frac{1}{2} e^{-|\mathbf{i}-\mathbf{j}|/\zeta} + (M^x)^2 \quad (3.11)$$

where  $M^x$  is the long-range order, such that  $\xi = (e^{\frac{1}{\zeta}} - 1)^{-1} \sim \zeta$ .

The excitation energies are calculated using the random phase approximation (RPA), which means that we assume that the excitations are small, harmonic fluctuations around the ground-state solution. This leads to a linear eigenvalue problem, [7] which is solved numerically. We can study the RPA spectrum, since the second-order derivatives are available for the functional, which is stored quasi-analytical for the high-order numerical calculations. At the phase transition the excitation energy goes to zero for a second-order phase transition, however, we know from NCCM [3] that the vanishing excitation energy is also the generic behavior at a termination point. Similar behavior could occur for ECCM.

## IV. NUMERICAL RESULTS

Usually, there is not much to be gained from studying the ground-state energy in great detail with the purpose of examining the performance of a method. Its convergence is much faster than that of any other quantity, and generally it is not an indication of the accuracy of the ground-state wave function. Moreover, for the transverse Ising model there is no value  $\lambda$ , where the numerical value of the energy is of specific interest. The position of the phase transition,  $\lambda_c$ , the only candidate for a point of interest, is not exactly known. The interested reader can contact us for precise numerical values for the ground-state energy. Instead, we focus on the excitation energy and the magnetization.

It is important to note that there are four specific cases studied here. Two different model states: the symmetry-broken, down-pointing ferromagnetic model state and the symmetry-preserved, sideways-pointing paramagnetic model state. These are two distinct approaches to the problem, which lead to two different numerical calculations. However, both can be studied, starting from both of the classical limits,  $\lambda = 0$  and  $\lambda = \infty$ . The one-body terms, from the SUB1 calculation, allow us to rotate each state from the model state to the starting state, which leads to some unexpected differences, which are summarized in Table I.

The ferromagnetic model state, which breaks the  $Z(2)$  symmetry, generally does much worse than the paramagnetic model state. We consider the two classical states that can arise with the paramagnetic model state. Firstly, the starting state at  $\lambda = 0$  breaks the  $Z(2)$  symmetry since it has  $M^z = 1$ . However, following this solution for the

ground state for increasing  $\lambda$ , it turns back and connects up with the symmetry partner;  $M^z \rightarrow -M^z$ , and ends at the starting value  $\lambda = 0$ , but now at with  $M^z = -1$ . At low orders this is a smooth transition, where  $M^z$  goes to zero, however, at high orders it jumps at a finite value of  $M^z$  to  $-M^z$ . At this point the excitation energy vanishes, for any order of approximation. Therefore both symmetry partners of the ground state are exactly degenerate and part of one continuous solution.

Secondly, starting with the paramagnetic model state at large values of  $\lambda$ , we find that the  $M^z$  remains zero, so the symmetry is never broken. This solution crosses the symmetry-broken solution as the latter turns back at  $M^z = 0$  and  $\lambda_c$ . However, looking at the excitation energy of the symmetry preserving solution, it tends to zero on the square lattice (see Fig. 2), but remains finite on the linear chain (see Fig. 3), signaling different behavior. Moreover, the ground-state solution continues beyond the point where the excitation energy goes to zero, therefore this behavior is not associated with the possible generic behavior at the termination point. The value of  $\lambda_c$ , where the excitation energy vanishes, is lower than the termination point of the solution with the paramagnetic model state starting from  $\lambda = 0$ .

The results from the square-lattice case (see Fig. 4 and Table II) are in greater agreement with those from other methods than the linear-chain results (see Fig. 5 and Table III) are with the exact results. Although this is to be expected, as the large quantum fluctuations on the linear chain is numerically difficult to deal with. Our most accurate means of determining the critical coupling constant is with the paramagnetic model state starting from the ferromagnetic limit  $\lambda = 0$ . It yields a value of  $\lambda_c = 3.014$  which is close to the best high-temperature series expansion results [10] of  $\lambda_c = 3.0441(4)$  and the best low-temperature series expansion results [11] of  $\lambda_c = 3.041(3)$ . Note that the series expansions, respectively, use the ferromagnetic and the paramagnetic model state. Other methods find similar, although less accurate results. [12] The details are summarized in Table II.

To investigate the model-state dependence further, we look at angles  $\theta$  in between the ferromagnetic angle  $\theta = 0$  and the paramagnetic angle  $\theta = -\frac{\pi}{2}$ . The largest angle at which the  $M^z$  does not jump is rather close to the ferromagnetic angle. The  $M^z$  for these different model states are shown in Fig. 6. Note that this solution continues to  $\lambda \rightarrow \infty$  because the  $Z(2)$  symmetry of the model state is broken. A continuous solution that traverses across the phase transition might be in high demand, however, the solutions, from a canted angle model state, do not have the right properties as the excitation energy becomes complex before the phase-transition point.

The correlation length increases in the vicinity of the phase transition (see Fig. 7), and shows good convergence. However, whether the correlation length is diverging at the phase transition is not clear. For the linear-chain case there are some indications of a sudden increase. More interestingly, for lower-order approximations, the maximum correlation length occurs before the termination point, and, as the order increases, the termination point and the extremum in the correlation length converge.

## V. CONCLUSIONS

The purpose of studying the transverse Ising model with the ECCM was to gain further knowledge of the optimal approach for its implementation before tackling more complicated physical models. Two major considerations came to light: the pivotal importance of the model state in the CCM calculation and that, importantly, the ECCM is the version of the CCM which can show symmetry breaking. Encouragingly, the ECCM SUB2 numerical results are accurate in comparison to other numerical techniques and is in agreement with the series expansion result [10,11] for  $\lambda_c$  on the square lattice.

The calculations in this paper necessitates the inclusion of the full ECCM SUB1 part of the functional, something we avoided in earlier work [4] because of the computational difficulties. However, the advantages of this inclusion are clear, since it allows us to study both phases in one consistent approach. Unfortunately, the order of approximation to which this calculation can be pursued is lower, because of the greater complexity. However, in the case of the transverse Ising model high-order approximations are not important since the convergence is good, and apart from the results for correlation length we have fully converged results within the SUB2 approximation, at SUB2-20.

The fact that the optimal ECCM SUB2 solution terminates in the critical region reveals that further improvements are necessary. Using more complicated model states, *i.e.*, a dimerized paramagnetic model state, could improve the situation. It seems that ECCM can only be implemented efficiently in the SUB2 truncation scheme, which is a serious drawback. However, a new approximation scheme has recently been developed, [3] which employs “block-spin model states” within the auspices of the SUB2 scheme. Advantageously, this scheme can be viewed as a way of performing a re-summation of the diagrams arising from the usual single-spin model states and as such can allow the inclusion of a great-many correlations. The formulation of an algorithm [3] for this scheme further increases its viability via computerization.

## ACKNOWLEDGMENTS

One of us (J.R.) gratefully acknowledges support for this work in the form of a research grant from the Engineering and Physical Sciences Research Council (EPSRC) of Great Britain. We like to thank Damian Farnell for the use of his NCCM, CBF, and VQMC results, and one of us (N.E.L.) likes to thank Niels Walet for some useful discussions.

- [1] N.E. Ligterink, N.R. Walet, and R.F. Bishop, *Ann. Phys. (N.Y.)*, **267**, 97 (1998).
- [2] N.D. Mermin and H. Wagner, *Phys. Rev. Lett.* **17**, 1133 (1966); Coleman, *Comm. Math. Phys.* **31**, 259 (1973).
- [3] J. Rosenfeld, Ph.D. thesis, UMIST, Manchester (1999).
- [4] J. Rosenfeld, N.E. Ligterink, and R.F. Bishop, *Phys. Rev. B* **60**, 4030 (1999).
- [5] E. Lieb, T. Schultz, and D. Mattis, *Ann. Phys. (N.Y.)* **16**, 407 (1961).
- [6] B.K. Chakrabarti, Amit Dutta, and P. Sen, *Quantum Ising Phases and Transitions in the Transverse Ising Model*, Lecture Notes in Physics **M41**, Springer, Berlin, 1996.
- [7] J.S. Arponen, *Ann. Phys. (N.Y.)* **151**, 311 (1983).
- [8] R.F. Bishop, *Theor. Chim. Acta* **80**, 95 (1991).
- [9] Y. Xian, in *Condensed Matter Theories*, edited by M. Casas, M. de Llano, J. Navarro, and A. Polls (Nova Science, Commack, New York), Vol. **10**, p.541.
- [10] H.-X. He, C.J. Hamer, and J. Oitmaa, *J. Phys. A* **23**, 1775 (1990).
- [11] J. Oitmaa, C.J. Hamer, and Zheng Weihong, *J. Phys. A* **24**, 2863 (1991).
- [12] R.F. Bishop, D.J.J. Farnell, and M.L. Ristig, in *Condensed Matter Theories*, Vol. **14**, (1999) (in press); *Ab Initio Treatments of the Ising Model in a Transverse Field*, R.F. Bishop, D.J.J. Farnell, and M.L. Ristig (to be published); M.L. Ristig and J.W. Kim, *Phys. Rev. B* **53**, 6665 (1996).

$$\begin{aligned}
 \mathbf{H} = -\lambda & \left[ \begin{array}{c} k + k'' + k'' \quad \diagdown \quad -k''k^2 - 2k''^2k \quad \diagdown \\ -2k \quad \diagup \quad -k''^3 \quad \diagup \quad -2k'' \quad \diagup \quad -k'' \quad \diagup \end{array} \right] - d \left[ \begin{array}{c} 1 - 4k''k + 4k''^2k^2 - 4k''^2 \quad \diagdown \quad + 8k''^3k \quad \diagdown \\ + 4k^2 \quad \diagup \quad + 8k''^3k \quad \diagup \quad -4 \quad \diagup \quad + 8k''k \quad \diagup \\ + 8kk'' \quad \diagdown \quad + 4k''^4 \quad \diagdown \quad + 4k''^2 \quad \diagdown \\ + 8k''^2 \quad \diagup \quad + 4 \quad \diagup \quad + 8k''^2 \quad \diagup \\ + 4k''^2 \quad \diagdown \quad + 4 \quad \diagdown \quad + 4 \quad \diagdown \end{array} \right]
 \end{aligned}$$

FIG. 1. The diagrams arising from the transverse Ising model functional with the ECCM SUB2- $n$  scheme, which yields the ground-state energy, where  $d$  is the dimensionality of the hyper-cubic lattice and  $\lambda$  is the external magnetic field.

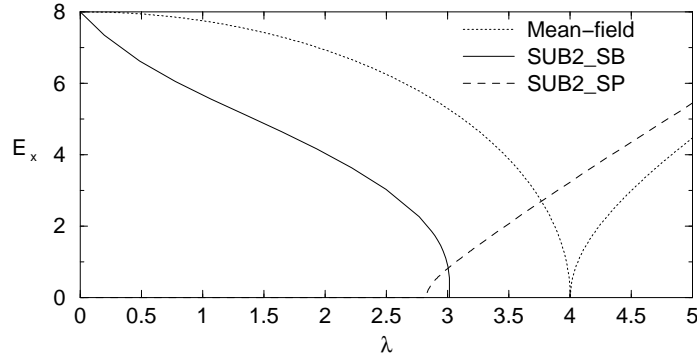


FIG. 2. The excitation energy,  $E_x$ , as a function of the transverse magnetic field,  $\lambda$ , on the square-lattice case from the ECCM SUB2- $n$  scheme with the paramagnetic model state and a mean-field calculation.

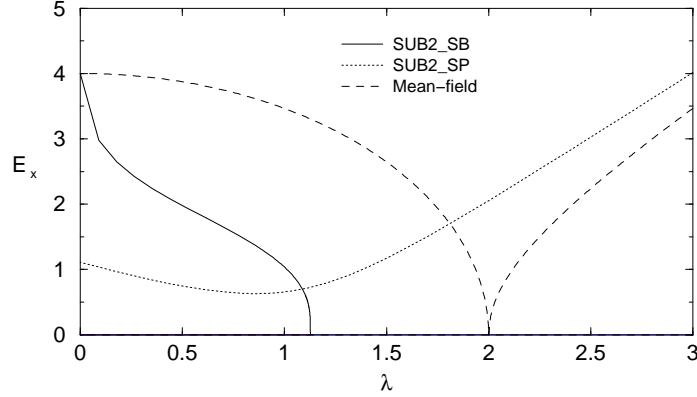


FIG. 3. The excitation energy,  $E_x$ , as a function of the transverse magnetic field,  $\lambda$ , on the linear-chain case from the ECCM SUB2- $n$  scheme with the paramagnetic model state and a mean-field calculation.

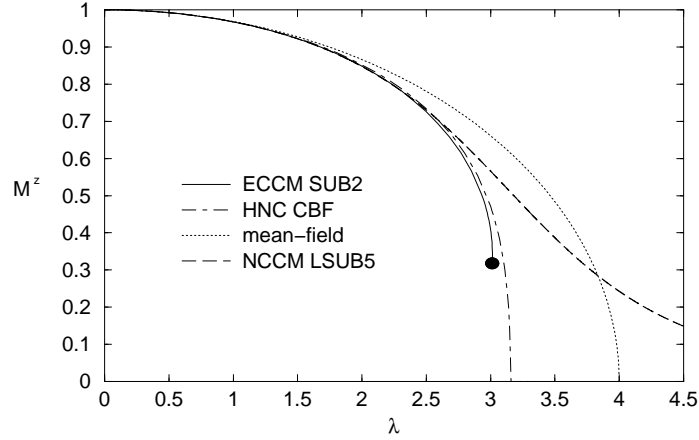


FIG. 4. The longitudinal magnetization,  $M^z$ , as a function of the transverse magnetic field,  $\lambda$ , on the for the linear-chain case from the ECCM SUB2- $n$  scheme with the paramagnetic model state, the highest-order NCCM LSUB $n$  scheme with the ferromagnetic model state, a mean-field calculation, and the exact solution. The LSUB $n$  truncation scheme retains only multiconfigurational creation operators in a localized area of  $n$  contiguous sites.



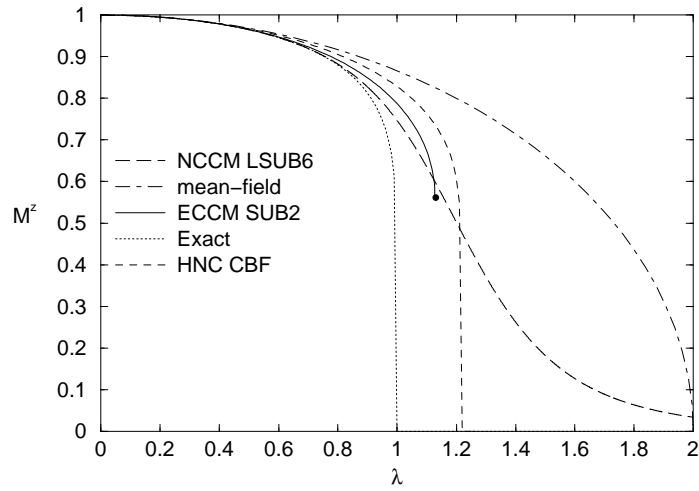


FIG. 5. The longitudinal magnetization,  $M^z$ , as a function of the transverse magnetic field,  $\lambda$ , on the for the linear-chain case from the ECCM SUB2- $n$  scheme with the paramagnetic model state, the highest-order NCCM LSUB $n$  scheme with the ferromagnetic model state, a mean-field calculation, and the exact solution.

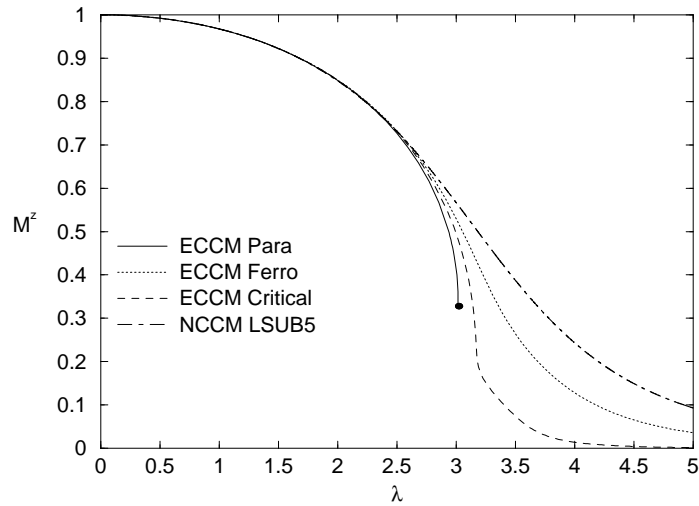


FIG. 6. The longitudinal magnetization,  $M^z$ , as a function of the transverse magnetic field,  $\lambda$ , on the square-lattice case from the ECCM SUB2- $n$  scheme with the paramagnetic model state, a critical canted model state, which allows the solution to be continuous, and the ferromagnetic model state.

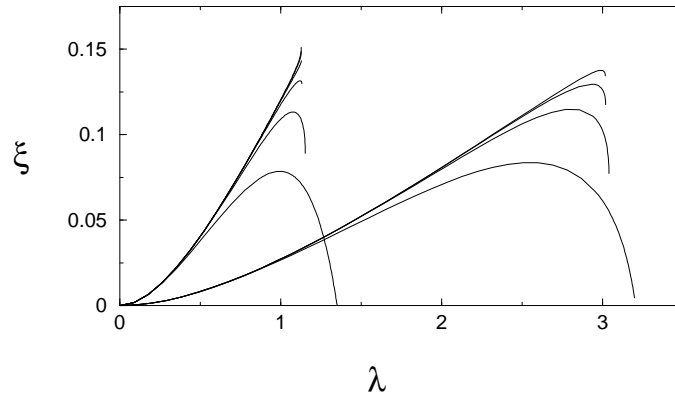


FIG. 7. The correlation length  $\xi$  as function of the coupling constant  $\lambda$ , for both the linear-chain case (left) and the square-lattice case (right) with increasing orders of approximation. For the linear-chain case the correlation length is converged, however, not completely so for the square-lattice case. For the square-lattice case, each line represents an approximation, where all correlators in a square, with lengths: 1, 2, 3, and 4, are taken into account, corresponding to 2, 5, 9, and 14 distinct correlators.

TABLE I. A summary of the main features for the square-lattice case, with different model states and different starting points. The qualitative difference with the linear-chain case is only for the excitation energy for the paramagnetic model state starting from large  $\lambda$ .

starting value	paramagnetic model state	ferromagnetic model state
$\lambda = 0$ $\lambda \uparrow$	solution terminates $E_x$ vanishes $M^z$ terminates	solution continues $E_x$ turns complex $M^z$ decreases
$\lambda = \infty$ $\lambda \downarrow$	solution continues $E_x$ vanishes $M^z = 0$	solution continues $E_x$ turns complex $M^z$ increases

TABLE II. A comparison of the critical value of the external magnetization at which various techniques determine the presence of a phase transition on the square lattice.

	VQMC <sup>a</sup>	HNC CBF <sup>a</sup>	HT Series Expansion <sup>b</sup>	LT Series Expansion <sup>c</sup>	ECCM SUB2
$\lambda_c$	$3.15 \pm 0.05$	3.12	3.0441(4)	3.041(3)	3.014

<sup>a</sup> Reference [12]

<sup>b</sup> Reference [10]

<sup>c</sup> Reference [11]

TABLE III. A comparison of the critical value of the external magnetization at which various techniques determine the presence of a phase transition on the linear chain.

	VQMC <sup>a</sup>	HNC CBF <sup>a</sup>	Exact	ECCM SUB2
$\lambda_c$	1.206	1.22	1.0	1.12

<sup>a</sup> Reference [12]